RSC Advances

ROYAL SOCIETY OF CHEMISTRY

www.rsc.org/advances

Porous Solid Acid with High Surface Area Derived from Emulsion Templating and Hypercrosslinking for Efficient Conversion of One-Pot Cellulose to 5-Hydroxymethylfurfural

Jianming Pan[a*], Heping Gao[a,b], Yunlei Zhang[a], Jun Zeng[a,b], Weidong Shi[a*], Changhua Song[a], Yongsheng Yan[a], Longbao Yu[a], Dandan Chang[a]

[a] School of Chemistry and Chemical Engineering, and Jiangsu University, Zhenjiang 212013, China

[b] School of Environmental and Chemical Engineering, and Jiangsu University of science and technology , Zhenjiang 212003, China

Abstract

This work addressed efficient conversion of one-pot cellulose to 5-hydroxymethylfurfural by porous solid acid in the presence of 1-ethyl-3-methyl-imidazolium chloride ([Emim]Cl). Based on stable water-in-oil Pickering high internal phase emulsions (HIPEs), porous solid acid (HC-PDVB-SS-SO_3H) was prepared by polymerizing divinylbenzene (DVB) and sodium p-styrenesulfonate (SS), succedent sulfonation in H_2SO_4 and hypercrosslinked process. HC-PDVB-SS-SO_3H with stable network exhibited mesopores within macropores structure, high BET specific surface area and more super-strong acid sites. To test catalytic activity, the reaction conditions were optimized via response surface methodology, and the sequence of the three variables affecting HMF yield followed the order temperature > reaction time > amount of catalyst. By comparing with the other as-prepared porous solid acid, it can also be concluded that BET specific surface area and super-strong acid site both played key roles in cellulose conversion. Moreover, HC-PDVB-SS-SO_3H was very easily reused at least four times without significant loss of activity.

Keywords: Cellulose; HMF; High surface area; Pickering HIPEs; Porous solid acid

1. Introduction

Although today coal, natural gas, petroleum, and other non-renewable fossil resources supply most of energy and chemicals,[1] in the future decades these fossil resources are unlikely to meet the growing needs of humanity. Meanwhile, consumers and governments paid more and more attention to environmental issues and environment protection are demanding renewable energy and products. With the development of conversion technology, abundant biomass resources have the potential to occupy the main position as feedstocks, particularly as renewable carbon sources for production fuels and chemicals.[2] One of those, the platform chemical 5-hydroxymethylfurfural (HMF) play important role in the biobased energy, because HMF can be converted by effective methods into many useful acid such as levulinic acid, 2,5-furandicarboxylic acid (FDA), and 5-hydroxy-4-keto-2-pentenoic acid,[3] as well as the promising fuel 2,5-dimethylfuran (DMF).[4] Most efforts toward HMF production have used the edible carbohydrate-based biomass such as fructose and glucose, which are easy to convert into valuable products. But their consumption for the manufacture of biofuels would cause a food deficiency, contrary to the case of wood-based biomass (e.g., cellulose).[5, 6] Unfortunately, improving the efficiency in cellulose convert into HMF is a challenge owing to the complex structure and difficulty for dissolving in general solvents.

In recent years, many studies have adopted many kinds of solid acid catalysts for the conversion of cellulose to HMF in ionic liquid because of solid acid and ionic liquid possessed ultra strong acid strength and unique solubility for cellulose. For example, we fabricated two acid-chromic chloride bi-functionalized solid acid catalysts by grafting the -SO_3H and Cr(III) onto the surface of treated

* Corresponding author. Tel.: +086 88791708; fax: +086 88791800.
E-mail address: pjm@ujs.edu.cn (J.M. Pan), shiwd999@163.com (W.D.Shi)

attapulgite (ATP) and halloysite nanotubes (HNTs), and their catalytic activities were evaluated for the conversion of one-pot cellulose to 5-hydroxymethylfurfural (HMF) in an ionic liquid 1-ethyl-3-methyl-imidazolium chloride ([EMIM]-Cl).[7] Very recently, we applied precipitation polymerization and Pickering emulsion polymerization combined with sulfonation process for synthesizing two kinds of polymeric solid acid for cellulose conversion in [EMIM]-Cl, which showed the satisfied yield of HMF.[8] Nevertheless, solid acids which show high yield of HMF as well as simple synthesis process in combination with easy recovery are also practically unavailable.

Recently, mesoporous solid acids[9-13] have been widely used in HMF production, due to their high specific surface area and large pore volume. For example, Clayton et al.[14] successfully obtained 29% of HMF yields by using a fixed bed porous metal oxide-based catalytic process in two liquid phases. Peng et al.[15] have prepared acidic large-pored mesoporous silica nanoparticles for catalysis of one-pot cellulose to HMF with low yield of 18%. Xiao's group successfully designed and synthesized of stable mesoporous polymeric solid acid for cellulose conversion.[16] The excellent catalytic activity was found for these mesoporous materials, but extra isolation steps for catalyst recycling mass and slow mass transfer to the active sites on the internal surface limited their further application.[17] The mass transport limitations of mesoporous solid acid can be overcome by using macroporous polymers based on high internal phase emulsions (HIPEs), which possess very large pores (1-100 um).[18] HIPEs, as emulsions with a volume fraction of the droplet phase higher than 74 %, provide a very convenient route to synthesize macroporous polymer supports (polyHIPEs) by polymerizing the monomers in the continuous phase.[19] However, conventional polyHIPEs synthesized from surfactant stabilized HIPEs have poor mechanical properties and low surface area.[20] In the literature, it was shown that the poor mechanical properties usually observed for polyHIPEs can be improved by using particle reinforcements, and one of the typical ways was utilized particle-stabilized HIPEs templates (Pickering HIPEs) to produce macroporous polymers. Bismarck's group[21] made use of Pickering HIPEs incorporated with small amounts of non-ionic polymeric surfactant to form of macroporous polyHIPEs with an open porous structure. To debate the bottleneck of low surface area, an alternative technology is the development of extensive post polymerisation crosslinking of swollen or dissolved polymers, namely hypercrosslinking (HC).[22] Krajnc and co-workers[23] had successfully created micropores within macroporous monoliths by post polymerisation hypercrosslinking of styrene/divinylbenzene polyHIPEs. Their work demonstrated that hypercrosslinking process could significantly increase of BET surface area, while retained the macroporous morphology typical of polyHIPEs materials.

Herein, a series of porous polymerized solid acids were successfully designed and produced by W/O Pickering HIPEs template method and succedent hypercrosslinked process. Firstly, the as-prepared hydrophobic silica particles and span 80 were both used to stabilize W/O Pickering HIPEs with an internal phase volume ratio of 84.8%. Then, Pickering HIPEs of external phase containing divinylbenzene (DVB) monomer, and internal containing DVB when external phasecontaining sodium p-styrene sulfonate (SS) monomer were applied to fabricated porous materials PDVB and PDVB-SS, respectively. After sulfonation in 98% H_2SO_4, two porous polymerized solid acids PDVB--SO_3H and PDVB-SS-SO_3H were obtained. Moreover, the third solid acid HC-PDVB-SS-SO_3H was prepared by further hypercrosslinking reaction and sulfonation of PDVB-SS. Then, three polymerized solid acids were all characterized, and the catalytic activity of them were discussed in detail by optimizing the reaction time, temperature and catalysts loading amounts in catalyzing cellulose to HMF. HC-PDVB-SS-SO_3H with large surface area, ultra strong

acid strength and stable network possessed good recyclability and catalytic activity compared with PDVB-SO_3H and PDVB-SS-SO_3H.

2. Material and Methods

2.1. Materials

1-ethyl-3-methyl-imidazolium chloride ([EMIM]-Cl), cellulose (powder, ca. 50 micron), 5-hydroxymethylfurfural (HMF) (>99%), tetraethoxysilane (TEOS), divinylbenzene (DVB), 3-methacryloxypropyltrimethoxysilane (KH-570) were supplieded from Aladdin reagent CO., LTD (Shanghai, China). 2,2′-azobis (2-methyl-propionitrile) (AIBN, 99%), toluene, ethanol, methanol, n-hexane, Span 80, K_2SO_4, $FeCl_3$ (anhydrous), potassium persulfate (KPS), $NH_3 \cdot H_2O$ (25 wt%), sodium p-styrene sulfonate (SS), 1,2-dichloroethane and acetone were purchased from Sinopharm Chemical Reagent Co., Ltd. (Shanghai, China). All other chemicals were supplied by local suppliers and used without further purification.

2.2. Instruments and characterization

FT-IR spectra were measured by a Nicolet NEXUS-470 FTIR apparatus (U.S.A.). The morphology of the silica particles and as-prepared solid acid catalysts were characterized by field emission scanning electron microscopy (SEM, JSM-7100F). Energy Dispersive Spectrometer (EDS) were taken based on SEM instrument. XPS spectra were performed on a Thermo ESCALAB 250 with Al Kα radition at y = 901 for the X-ray sources, the binding energies were calibrated using the C_{1s} peak at 284.9 eV. Elemental coposition was recorded by the vario EL III elemental analyzer (Elementar, Hanau, Germany). The acidic features of samples were all measured according to NH_3 temperature-programmed desorption (NH_3-TPD) curves, which were recorded by thermal conductivity detector (TCD, DAS-7000, Beijing, China). TGA of samples were performed for powder (near 10 mg) using a Diamond TG/DTA instruments (Perkin-Elmer, U.S.A.) under a nitrogen atmosphere up to 800 ^oC with a heating rate of 5.0 ^oC min^{-1}. The water contact angle of silica particles were measured through the Optical Contact Angle Measuring Device (KSV CM200). Detailed test procedure was described as follow. 2.0 μL of deionized water was injected on the sample surface through the syringe pump, then the images of the water droplet were obtained using the camera in measuring device after the water droplet was formed on the sample surface about 30 s. Finally, these images were analyzed using the supplied software to determine the contact angle of sample.

2.3. Synthesis of hydrophobic silica particles as stabilizers

Hydrophobic silica particles, which were used to stabilize W/O Pickering HIPEs, were synthesized via two steps. Firstly, hydrophilic silica particles were prepared using the well-known hydrolysis and condensation reaction according to modified Stöber's method.[24] 6.0 mL of TEOS was slowly injected into uniform solution containing 90 mL of ethanol, 10 mL of H_2O and 3.14 mL of 25 wt% $NH_3 \cdot H_2O$. Then, the mixtures were reacted for 1.0 h at 30 ^oC under the mechanical stirring, and subsequently the reaction products were separated and washed by centrifugation for several times with ethanol. Finally, the uniform sizes of hydrophilic silica particles were obtained through drying for 8.0 h at 40 ^oC in vacuum drying oven.

Secondly, as-prepared hydrophilic silica particles were further modified by KH-570. As a typical run, hydrophilic silica particles (1.0 g), toluene (150 mL), H_2O (15 mL) and KH-570 (3.5 mL) were

mixed and stirred for 24 h at 40 °C in a 250 mL three-neck flask. Subsequently, the reaction products were separated and washed by ethanol. Finally, hydrophobic silica particles were obtained through drying for 12 h at 40 °C in vacuum drying oven.

2.4. Preparation of PDVB-SO_3H and PDVB-SS-SO_3H

PDVB-SO_3H was prepared by emulsion polymerization and subsequent sulfonation process. The first step was the synthesis of porous PDVB polymers via Pickering HIPEs template method, and the HIPEs recipes were listed in Table 1. A continuous phase was formed by stirring the hydrophobic silica particles (0.3 g), AIBN (0.04g), DVB (3.0 mL) and span 80 (0.4 mL) in a 100 mL three-neck flask. Afterwards, 16.8 ml of the internal aqueous phase comprised of K_2SO_4 (0.08 g) was gradually added into continuous phase under the continuous stirring, and the stable W/O Pickering HIPEs were obtained. Then, the obtained Pickering HIPEs were transferred into a plastic centrifuge tube and polymerized in a circulating air oven at 60 °C. After 12 h, the as-prepared PDVB were washed with deionized water and acetone in turn, and then macroporous PDVB monoliths were dried at 80 °C for 12 h. The second step was grafting the above PDVB with -SO_3H by sulfonation process. Briefly, PDVB monoliths (1.0 g) and 98% H_2SO_4 (30 mL) were mixed and stirred at 70 °C for 12 h. Then, the reaction products were filtered and washed to remove the excess of H_2SO_4 by using amounts of deionized water. Finally, the PDVB-SO_3H were obtained after drying in vacuum at 80 °C for 3.0 h

The preparation of PDVB-SS-SO_3H also had two steps, such as the fabrication of macroporous PDVB-SS monoliths and subsequent sulfonation process. For the preparation of PDVB-SS, the SS (0.2 g) and KPS (0.04g) were added into the internal aqueous phase (Table 1), and the other processes were same as the formation of macroporous PDVB monoliths. Moreover, the sulfonation process was followed by the step described above. Finally, the obtained products were named as PDVB-SS-SO_3H.

2.5. Preparation of HC-PDVB-SS-SO_3H

The preparation of HC-PDVB-SS-SO_3H included the post polymerisation hypercrosslinking of PDVB-SS and subsequent sulfonation process. As a typical run, the as-prepared PDVB-SS (1.0 g) was swollen in 1,2-dichloroethane (40 mL) under N_2 for 3.0 h. Then, $FeCl_3$ (1.6 g) in 20 mL of 1,2-dichloroethane was added into the mixture of PDVB-SS and 1,2-dichloroethane, and the reaction mixture was stirred for another 18 hours at 80 °C. The resulting hypercrosslinked products were filtered and washed three times with water and methanol, and then washed with methanol in a Soxhlet extraction for 24 h. Subsequently, products (HC-PDVB-SS) were dried under vacuum at 40 °C for 24 h. Next, the sulfonation process of HC-PDVB-SS was followed by the step described above. Consequently, the obtained products were named as HC-PDVB-SS-SO_3H.

2.6. The conversion of cellulose to HMF and analysis of HMF

A typical procedure for the conversion of cellulose to HMF according to modified Wei's method,[25] which was detailed as follow. Firstly, cellulose (0.1 g) and [EMIM]Cl (2.0 g) was heated under the stirring at 125 °C for 30 min until a clear solution to destroy the degree of crystallization and regularity of the cellulose. Then, as-prepared HC-PDVB-SS-SO_3H (45 mg) was added into the mixed solution, and continued reacting for 2.0 h at 125 °C under continuous stirring. Next, the reaction products were quenched immediately with cold water, and diluted for 5000 times with deionized water. Finally, liquid samples were analyzed by a high performance liquid

chromatography (HPLC) with Agilent 1200. HMF was detected with a UV-Vis detector at wavelength of 283 nm. The column used was Agilent TC-C18 Column (4.6 × 250 mm, 5.0 mm). The mobile phase was the mixed water and methanol with the volume ratio for 30 : 70, and flow rate and column oven were set to 0.7 mL min^{-1} and 25 ^{o}C, respectively. Meanwhile, the HMF content was obtained according to the standard curve method. In this work, the HMF yield was defined as the ratio of total moles number of carbon atoms of HMF (n_1) and total moles number of carbon atoms in initial cellulose loaded in the reactor (n_0), which was expressed in Eq. (1).

$$Y_{\mathrm{HMF}}(\%) = 100 \times (n_1 / n_0) \quad (1)$$

3. Results and discussion

3.1. Fabrication of hydrophobic silica particles

The water contact angle images of hydrophilic and hydrophobic silica particles were shown in Fig. 1a and Fig. 1b, and it could be clearly observed that water contact angle of them were about 34.5 ° and 125.7°, respectively, suggesting that hydrophobic silica particles were successfully prepared by grafting vinyl groups to the surface of hydrophilic silica particles. Moreover, the proper water contact angle meet the requirement about stabilizing W/O Pickering HIPEs, which was proved by Binks's groups about using the particles with the water contact angle of 123 ° to stabilize W/O Pickering HIPEs.[26] Meanwhile, the morphology of hydrophilic and hydrophobic silica particles was both observed by SEM, which was shown in Fig. 2a and 2b, respectively. Hydrophilic and hydrophobic silica particles were both regular sphere-shaped, and their sizes were 200 ± 20 nm and 250 ± 20 nm, respectively. This phenomenon of increased sizes was further confirmed that the vinyl groups were grafted to the surface of hydrophilic silica particles.

3.2. Characterizations of porous polymerized solid acid

3.2.1. Morphological features and porous structure *of catalysts*

Fig. 2 also showed the SEM images of PDVB-SO_3H (c), PDVB-SS-SO_3H (d) and HC-PDVB-SS-SO_3H (e). Clearly, PDVB-SO_3H (Fig. 2c) displayed a well-defined open-cell structure (void size of 12 ± 2 μm) and interconnecting pore throat sizes in the range 0.5-3.0 μm. However, PDVB-SS-SO_3H (Fig. 2d) had close-cell structure with few interconnecting pore throats, and a polymer film covered region between two voids. The mechanism of pore throat formation in polyHIPEs may be the films for separation of the droplets in HIPEs must be sufficiently thin up to break and form pore throats.[27] Meanwhile, polymerized SS monomer layer in internal phase of PDVB-SS-SO_3H increased thickness of the contact domains between the neighboring droplets during polymerization, and the function against coalescence resulted in the close-cell structure. It was also found that the void size of PDVB-SS-SO_3H (30 to 50 μm) was larger than that of PDVB-SO_3H. It was possibly because dissolved SS monomers in the internal phase of PDVB-SS-SO_3H brought about high interfacial energy and low electric potential between oil/water interface, which was benefit for increasing the sizes of HIPEs droplets. Compared with PDVB-SS-SO_3H, no significant change in morphological features was observed for HC-PDVB-SS-SO_3H (Fig. 2e). This result was also investigated and proved by Krajnc's group. They suggested that post polymerisation crosslinking involved reactions between pre-formed polymer chains, and the morphological feature of the material was slightly affected.[17]

Porous structure has a remarkable effect on the catalytic effect, and then Nitrogen

adsorption-desorption isotherms of HC-PDVB-SS-SO_3H (a), PDVB-SS-SO_3H (b) and PDVB-SO_3H (c) were listed in Fig. 3. As shown in Fig. 3, they all displayed a typical type-IV isotherm with a step capillary condensation in the relative pressure range of 0.1-0.9, and this type of isotherm was in agreement with the presence of obviously mesoporosity. Meanwhile, the porosity property of HC-PDVB-SS-SO_3H, PDVB-SS-SO_3H, and PDVB-SO_3H were listed in Table 2. Clearly, the BET surface area (323.95 m^2 g^{-1}) and pore volume (0.20 cm^3 g^{-1}) of HC-PDVB-SS-SO_3H were obviously higher than those of PDVB-SS-SO_3H (80.06 m^2 g^{-1}, 0.13 cm^3 g^{-1}), and PDVB-SO_3H (30.24 m^2 g^{-1}, 0.05 cm^3 g^{-1}), respectively. The low surface area was found for highly permeable macroporous PDVB-SO_3H polymers, and this result demonstrated that PDVB-SO_3H possessed very low amount of mesopores. Although close-cell structure was obtained for HC-PDVB-SS-SO_3H, significant enlargement of the amount of mesopores in the material was found resulting from post polymerisation hypercrosslinking. Nevertheless, BJH pore diameter (5.94 nm) of HC-PDVB-SS-SO_3H was lower than that of PDVB-SS-SO_3H (10.67 nm), and PDVB-SO_3H (14.19 nm), respectively, which could be attributed to the presence of SS monomers might block the mesopores and increase the density of the network in the hypercrosslinking process.

3.2.2. Chemical composition of catalysts

Fig. 4 showed the FT-IR spectras of PDVB-SO_3H (a), PDVB (b), regenerated HC-PDVB-SS-SO_3H (c), HC-PDVB-SS-SO_3H (d) and PDVB-SS-SO_3H (e), respectively. The peaks at 1456 cm^{-1} associated with benzene ring, and 1107 cm^{-1} assigned to Si–O–Si antisymmetric stretching vibration could both be clearly found in the all samples,[28] suggesting the presecce of silica particles and monomers such as DVB or SS. Additionally, peaks of 1039 cm^{-1} attributed to C-S bond, and 1170 cm^{-1} belonged to -SO_3H group were also clearly observed in the samples of PDVB-SO_3H, regenerated HC-PDVB-SS-SO_3H, HC-PDVB-SS-SO_3H and PDVB-SS-SO_3H, declaring that the sulfonic group were successfully grafted to the benzene rings of monomers.

Energy dispersive spectrometer (EDS) analysis for PDVB, PDVB-SO_3H, and PDVB-SS-SO_3H were listed in Fig. 5a-5c, respectively. When compared Fig. 5a with Fig. 5b, the peak of element S appeared in the sample of PDVB-SO_3H, and same phenomenon was also found in the sample of PDVB-SS-SO_3H when compared Fig. 5a with Fig. 5c, which suggested that -SO_3H groups were successfully grafted to the surface of PDVB via sulfonation process. Furthermore, it could be found that the peak of element S in the sample of PDVB-SS-SO_3H was stronger than that of PDVB-SO_3H, and the amount of S was also more than that of PDVB-SO_3H. Thus, it could be emphasized that PDVB-SS-SO_3H had a PSS layer which resulted in more -SO_3H groups in the sample of PDVB-SS-SO_3H. Additionally, the results of element analysis for PDVB, PDVB-SO_3H and PDVB-SS-SO_3H were all shown in the corresponding figures, respectively. What's more, the weight of S in the sample of PDVB-SO_3H (0.65 %) was increased to 2.28 % in the sample of PDVB-SS-SO_3H, and S element did not exist in PDVB. Therefore, these results were same as the results of EDS analysis.

Fig. 6 showed the X-ray photoelectron spectroscopy (XPS) measurements of PDVB-SO_3H and HC-PDVB-SS-SO_3H, respectively. Clearly, PDVB-SO_3H and HC-PDVB-SS-SO_3H both showed the signals of S, C, Si and O, possible indicating the presence of -SO_3H group and hydrophobic silica particles in these samples. Correspondingly, the high resolved XPS spectrum of C1s showed the signals at around 284.7 eV, which was associated with C-S bond in these samples. This result further proved the successful introduction of -SO_3H into the network of these samples, and -SO_3H groups

would contribute to increase the acid strength of these solid acids.[29]Moreover, the signal of S2p of PDVB-SO_3H and HC-PDVB-SS-SO_3H were found in same position with binding energy 169 eV, suggesting hypercrosslinked process of HC-PDVB-SS-SO_3H had no obvious effect to the introduction of -SO_3H groups, and the results also supported the fact that the HC-PDVB-SS-SO_3H catalyst possessed rigid network structure and good chemical stability. Meanwhile, the peak position of Si2p of PDVB-SO_3H and HC-PDVB-SS-SO_3H were both at 102.2 eV, and the phenomenon showed that hydrophobic silica particles might not be involved in other reactions except to emulsifying process.

Fig. 7 showed the TGA curves of PDVB-SO_3H (a), HC-PDVB-SS-SO_3H (b), and PDVB-SS-SO_3H (c), respectively. Slight weight losses of PDVB-SO_3H (6.78%), HC-PDVB-SS-SO_3H (9.09%) and PDVB-SS-SO_3H (11.29%) within the initial temperature range (< 150 ^oC) could be observed, respectively, which could be attributed to the loss of the H_2O in these samples.[30] With the temperature increased to 450 ^oC, the obvious weight losses of PDVB-SO_3H (11.37%), HC-PDVB-SS-SO_3H (16.57%), and PDVB-SS-SO_3H (17.64%) resulted from decomposition of -SO_3H groups could also be seen, respectively.[31]Interestingly, it could be found that the more -SO_3H groups catalyst had, the higher adsorption content of water, which suggested that -SO_3H groups provided more hydrophilic surface. When the temperature further increased to 800 ^oC, PDVB-SO_3H, HC-PDVB-SS-SO_3H and PDVB-SS-SO_3H had a significant weight loss with 46.75%, 36.76%, and 30.76%, respectively, due to the destruction and decomposition of spatial structure of catalysts. At 800 ^oC, the remaining mass for catalysts may be put down to rigid silica particles and residual carbon by calcining polymers.[32]

3.2.3 The acidic properties of catalysts

The acidic features of PDVB-SO_3H, PDVB-SS-SO_3H and HC-PDVB-SS-SO_3H catalysts were determined by means of NH_3-TPD, respectively. Additionally, the type of distinguishing acid sites was based on desorption temperatures of NH_3, and 150-250 ^oC, 250-350 ^oC, 350-500 ^oC and >500 ^oC were measured as weak, medium, strong and super-strong of the acid sites, respectively.[33] As shown in Fig. 8, it can be clearly seen that medium, strong and very strong acid sites existed in PDVB-SO_3H and PDVB-SS-SO_3H, but HC-PDVB-SS-SO_3H possessed only super-strong acid sites can also be obvious observed. Moreover, the areas of the peak represented the amount of acidic sites were further calculated and summarized in Table 2, respectively. The total acidic amount of PDVB-SO_3H for 235 μmol g^{-1} (i.e. respective acidic amounts of 50 μmol g^{-1}, 116 μmol g^{-1} and 69 μmol g^{-1} for the acidic strengths of 250 ^oC, 378 ^oC and 557 ^oC) was less than that of PDVB-SS-SO_3H for 313 μmol g^{-1} (i.e. respective acidic amounts of 49 μmol g^{-1}, 95 μmol g^{-1} and 169 μmol g^{-1} for the acidic strengths of 285^oC, 369 ^oC and 518 ^oC), and HC-PDVB-SS-SO_3H for 237 μmol g^{-1} (i.e. respective acidic amounts of 104 μmol g^{-1} and 133 μmol g^{-1} for the acidic strengths of 604 ^oC and 706 ^oC), respectively. What's more, it could also be simply proved that results of total acidic amount were identical with the amounts of -SO_3H groups resulting from TGA analysis. Meanwhile, the acidic amount provides many acidic sites which can help to improve efficiency for conversion of cellulose into HMF.[34]Therefore, 185 μmol g^{-1} of strong acid sites at 378 ^oC and 557 ^oC for PDVB-SO_3H, 264 μmol g^{-1} of strong acid sites at 369 ^oC and 518 ^oC for PDVB-SS-SO_3H, and 237 μmol g^{-1} of super-strong acid sites at 604 ^oC and 706 ^oC for HC-PDVB-SS-SO_3H were effective to catalyze cellulose into HMF. Furthermore, the fact that strong acid sites palyed a key factor for cellulose conversion was tested in our recent work.[8] Thus, HC-PDVB-SS-SO_3H would posess

predominant catalytic activity then PDVB-SO_3H and PDVB-SS-SO_3H, owing to the more strong acid sites. These results supported that HC-PDVB-SS-SO_3H was selected in the further catalytic activity studies.

3.3. Conversion of cellulose to HMF

The experimental data of correlation of three variables, such as catalyst dosage (*m*, mg), temperature (*T*, ^oC) and reaction time (*t*, h), were fitted using a low-order polynomial equation to evaluate the effect of each independent variable on the response. Meanwhile, in this work, the conversion efficiency was evaluated by the analysis of variance (ANOVA) with the HMF yield (*Y*, mol %) as the response, and final obtained equation of HC-PDVB-SS-0-SO_3H in terms of the actual factors was expressed in Eq. (2).

$$Y = -666.19 + 9.36T + 52.94t + 1.47m - 0.3Tt - 4.96\times10^{-3}Tm - 0.04tm - 0.03T^2 - 3.37t^2 - 6.34\times10^{-3}m^2 \quad (2)$$

The 3D response surface and the 2D contour plots showing the effects of three variables for HC-PDVB-SS-SO_3H catalyst on HMF yield were displayed in Fig. 9. The interaction between amount of catalyst and temperature on HMF yield under constant reaction time (1.75 h) were shown in Fig. 9a and Fig. 9b, respectively. With the increase of amount of catalyst and temperature, it obvious observed that HMF yield showed a trend of rapid increase in the beginning stages, then reaching the maximum, and finally reducing with more catalyst and higher temperature used. The phenomenon may be ascribed to the following reasons. Firstly, the increasing reaction temperature and amount of catalyst reduced the viscosity of ionic liquids and increased contact area between catalyst and the reactants, which was benefit to accelerate the degradation of cellulose.[35] Secondly, the produced HMF covered the acid sites of catalysts, and the conversion of HMF into other tarry substances such as insoluble humines and soluble polymers by the polymerization and cross-polymerization of HMF were enhanced with the further increasing reaction temperature and amount of catalyst.[36] Additionally, Qu's groups also presented same results.[37] Meanwhile, many researchers also reported the fact that by-products formic acid and levulinic acid could be examined by HLPC in this process.[38, 39] Interestingly, the same phenomenon was also found in Fig. 9c and Fig. 9d, as well Fig. 9e and Fig. 9f, which indicated that the bidirectional interaction between variables such as reaction time and amount of catalyst at 125 ^oC, reaction time and temperature with 45 mg catalyst were also important terms in the production of HMF from cellulose. Moreover, the sequence of the three variables affecting HMF yield followed the order temperature > reaction time > amount of catalyst, which was easyly obtained according to the number of crosslinking of the contour plots with coordinate axis of Fig. 9b, Fig. 9d and Fig. 9f, respectively. The optimal condition achieved by the response surface methodology was 0.10 g cellulose, 45 mg of catalyst, temperature of 125 ^oC, and reaction time of 1.75 h. The optimal HMF yield of 28.9% was closer to the experimental value of 29.2%, implying that predication way were reasonable and credible.

In order to discuss the influence of performance of materials on the conversion of cellulose into HMF, the optimal HMF yield of PDVB-SO_3H (22.3%) and PDVB-SS-SO_3H (25.2%) in same condition (50 mg of catalyst, 2.0 h of reaction time and 130 ^oC of reaction temperature) by using same analysis method were obtained, which were also listed in Table 2, respectively. It was clearly found that HC-PDVB-SS-SO_3H obtained higher HMF yield than that of the other two catalysts. BET specific surface and super-strong acid site were considered to be hold responsible for the excellent

performance of HC-PDVB-SS-SO_3H. Firstly, higher BET specific surface area was helped to increase contact frequency between reaction substrates and catalytic acid sites. Secondly, more super-strong acid site was more conducive to improve the catalytic effect of cellulose to HMF than other type of acid sites. Moreover, HMF yield of PDVB-SS-SO_3H was slightly higher than that of PDVB-SO_3H owing to the main advantages of BET specific surface area and total acidity. According to the above discussion about the performance of catalysts, it could be concluded that higher BET specific surface area and more super-strong acid sites of HC-PDVB-SS-SO_3H, as the remarkable effects, effetively facilitated the conversion of cellulose to HMF.

3.4. Regeneration of HC-PDVB-SS-SO_3H catalyst

The regeneration of catalyst was very important to the practical production of HMF, which was accorded with the demand of green and sustainable chemistry. Therefore, to evaluate the reusability of HC-PDVB-SS-SO_3H catalyst, recycling tests were conducted at the optimized reaction conditions. The results for the regeneration experiment were shown in Fig. 10. The solid acid catalysts HC-PDVB-SS-SO_3H were recovered by simply suction filtration using Hirsch funnel the mixture products diluted with deionized water after the first reaction end, washing them many times with a mixture of n-hexane and methanol, and drying at 30 ^oC for 24 h in a vacuum oven. Subsequently, recovered HC-PDVB-SS-SO_3H was used to catalyze cellulose into HMF for four times, and the yields of HMF were 28.7%, 27.5%, 27.4%, and 26.5%, respectively. It could be found that HMF yield slowly reduced. It was probably because the formation of by-product on the catalytic centers of HC-PDVB-SS-SO_3H that could not wash out in mixture of n-hexane and methanol, which limited the accessibility of new reactant molecules to the sulfonic acid sites. Yet, the HC-PDVB-SS-SO_3H catalyst still had a good activity after reusing for four times. Thus the porous Meanwhile, the FT-IR spectra of regenerated HC-PDVB-SS-SO_3H was similar with HC-PDVB-SS-SO_3H, especially the intensity of the peaks of Si-O-Si and -SO_3H groups (Fig. 4), indicating that the HC-PDVB-SS-SO_3H catalyst possessed rigid structure and stable acidic activity sites. The superior recyclability of HC-PDVB-SS-SO_3H came from their excellent chemical and mechanical stability of both acidic sites and polymer network, which were very important for their widely practical applications. These results, to some extent, suggested that the heterogeneous HC-PDVB-SS-SO_3H catalyst has the potential to be effectively recycled and reused for the dehydration reaction.

4. Conclusion

In this work, porous solid acid catalyst (HC-PDVB-SS-SO_3H) with high surface area was derived from Pickering HIPEs template and hypercrosslinking process. Then the production of HMF from cellulose using HC-PDVB-SS-SO_3H as catalyst in the presence of [EMIM]Cl was proved to be feasible, and obtained yield of HMF at 29.2% for HC-PDVB-SS-SO_3H at the optimized conditions. Moreover, the fact that the BET specific surface area and super-strong acid site of catalyst as the key factor than other three factors including temperature, time and catalyst loading was identified by ANOVA affecting the conversion efficiency. This work was the continue efforts for making stable polymeric solid acid, and the results from this work could be valuable for future research towards development of new reactors, especially their wide application for biomass and bioenergy.

Acknowledgements

This work was financially supported by the National Natural Science Foundation of China (no.

21107037, no.21176107, no. 21306013), Natural Science Foundation of Jiangsu Province (no.BK20131223), National Postdoctoral Science Foundation (no. 2013M530240), Special National Postdoctoral Science Foundation (no. 2014T70480), Postdoctoral Science Foundation of Jiangsu Province (no. 1202002B) and Programs of Senior Talent Foundation of Jiangsu University (no. 12JDG090).

References

1 J. C. Serrano-Ruiz and J. A. Dumesic, Energy Environ. Sci., 2011, 4, 83-99.
2 J.N. Chheda, G.W. Huber and J.A. Dumesic, Angew. Chem. Int. Ed., 2007, 46, 7164-7183.
3 A.A. Rosatella, S.P. Simeonov, R.F.M. Frade and C.A.M. Afonso, Green Chem., 2011, 13, 754-793.
4 F.W. Lichtenthaler, Acc. Chem. Res., 2002, 35, 728-737.
5 K. I-Jung, S. Norihiro, Y. Yusuke and C.W.W. Kevin, RSC Adv., 2013, 3, 2028-2034.
6 F.G. Calvo-Flores and J.A. Dobado, ChemSusChem, 2010, 3, 1227-1235.
7 Y.L. Zhang, J.M. Pan, M.Y. Gan, H.X. Ou, Y.S. Yan, W.D. Shi and L.B. Yu, RSC Adv., 2014, 4, 11664-11672.
8 Y.L. Zhang, J.M. Pan, Y.S. Yan, W.D. Shi, L.B. Yu, RSC Adv. 4(2014) 23797-23806.
9 N.L. Torad, M. Naito, J. Tatami, A. Endo, S.Y. Leo, S. Ishihara, K.C.W. Wu, T. Wakihara and Y. Yamauchi, Chemistry-An Asian Journal, 2014, 9, 759-763.
10 K. Na, M. Choi and R. Ryoo, Microporous and Mesoporous Materials, 2013, 166, 3-19.
11 Y.Y. Lee and K.C.W. Wu, Physical Chemistry Chemical Physics, 2012, 14, 13914-13917.
12 I.I. Ivanova and E.E. Knyazeva, Chemical Society Review, 2013, 42, 3671-3688.
13 I.J. Kuo, N. Suzuki, Y. Yamauchi and K.C.W. Wu, RSC Advances, 2013, 3, 2028-2034.
14 C.V. McNeffa, D.T. Nowlana, L.C.B. McNeffa and R.L. Fedieb, Energy Environ. Sci., 2012, 5, 7559-7574.
15 W.H. Peng, Y.Y. Lee, C. Wu and K.C.W. Wu, J. Mater. Chem., 2012, 22, 23181-23185.
16 F.J. Liu, A.M. Zheng, I. Noshadi and F.S. Xiao, Appl. Catal. B, 2013, 136, 193-201.
17 I. Pulko, J. Wall, P. Krajnc and N.R. Cameron, Chem. Eur. J., 2010, 16, 2350-2354.
18 H.F. Zhang and A.I. Cooper, Soft Matter, 2005, 1, 107-113.
19 B.H.L. Oh, A. Bismarck and M.B. Chan-Park, Biomacromolecules, 2014, 15, 1777-1787.
20 A.F. Gross and A.P. Nowak, Langmuir, 2010, 26, 11378-11383.
21 B.V.O. Ikem, A. Menner, T.S. Horozov and A. Bismarck, Adv. Mater., 2010, 22, 3588-3592.
22 M.G. Schwab, I. Senkovska, M. Rose, N. Klein, M. Koch and J. Pahnke, Soft Matter, 2009, 5, 1055-1059.
23 U. Sevšek, J. Brus, K. Jeřabek and P. Krajnc, Polymer, 2014, 55, 410-415.
24 W. Stöber, A. Fink and E. Bohn, J. Colloid Interface Sci., 1968, 26, 62-69.
25 H.H. Wei, Y.Y. Lee, W.H. Peng and K.C.W. Wu, Catalysis Today, 2011, 174, 65-69
26 B.P. Binks and S. Lumsdon, Phys. Chem. Chem. Phys., 2000, 2, 2959-2967.
27 A. Menner and A. Bismarck, Macromol. Symp., 2006, 242, 19-24 .
28 D.C. Niu, Z.J. Liu, Y.S. Li, F. Luo, J.Y. Zhang, J.P. Gong and J.L. Shi, Adv. Mater., 2014, 29, 4947-4953.
29 C. Koibeck, M. Killian, F. Maier, N. Paape, P. Wasserscheid and H.P. Steinrück, Langmuir, 2008, 24, 9500-9507.
30 L. Wang, H. Wang, F.J. Liu, A.M. Zheng, J. Zhang, Q. Sun, J.P. Lewis, L.F. Zhu, X.J. Meng and F.S. Xiao, ChemSusChem, 2014, 7, 402-406.
31 F.J. Liu, X.J. Meng, Y. L. Zhang, L.M. Ren, F. Nawaz and F.S. Xiao, J. Catal., 2010, 271, 52-58.
32 J.M. Pan, B. Wang, J.D. Dai, X.H. Dai, H. Hang, H.X. Ou and Y.S. Yan, J. Mater. Chem., 2012, 22, 3360-3369.
33 D. Liu, P. Yuan, H.M. Liu, J.G. Cai, D.Y. Tan, H.P. He, J.X. Zhu and T.H. Chen, *Appl. Clay Sci.,* 2013, 80, 407-412.

34 P. Kalita, B. Sathyaseelan, M.A. Javaid, S.M. Zaidi, M.A. Vinu, A. Chari, Chem. Eur. J. 2010, 16, 2843-2846.

35 A.I. Torres, P. Daoutidis and M. Tsapatsis, Energy Environ. Sci., 2010, 3, 1560-1572.

36 J.N. Chheda, Y. Roman-Leshkov and J.A. Dumesic, Green Chem., 2007, 9, 342-350.

37 Y.S. Qu, Q.Y. Wei, H.Q. Li, P. Oleskowicz-Popiel, C.P. Huang and J. Xu, Bioresource Technology, 2014, 162, 358-364.

38 E.I. Gürbüz, J.M.R. Gallo, D.M. Alonso, S.G. Wettstein, W.Y. Lim and J.A. Dumesic, Angew. Chem., 2013, 52, 1270-1274.

39 H.B. Zhao, J.E. Holladay, H. Brown and Z.C. Zhang, Science, 2007, 316, 1597-1600.

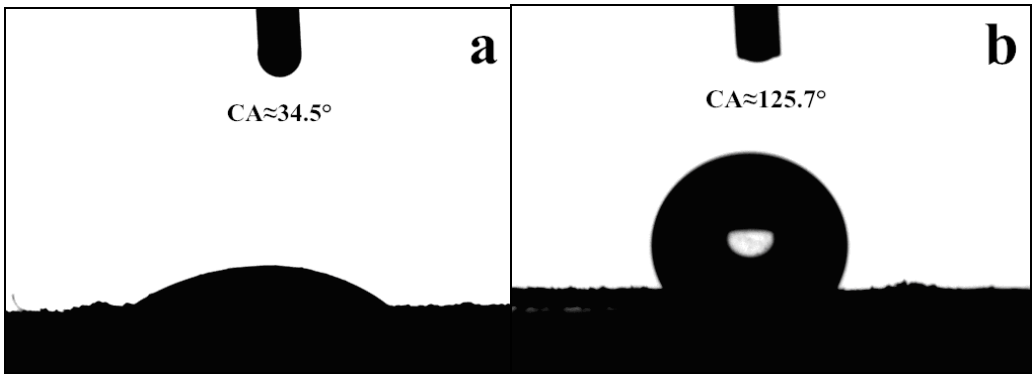

Fig. 1 Water contact angle images of hydrophilic (a) and hydrophobic (b) silica particles.

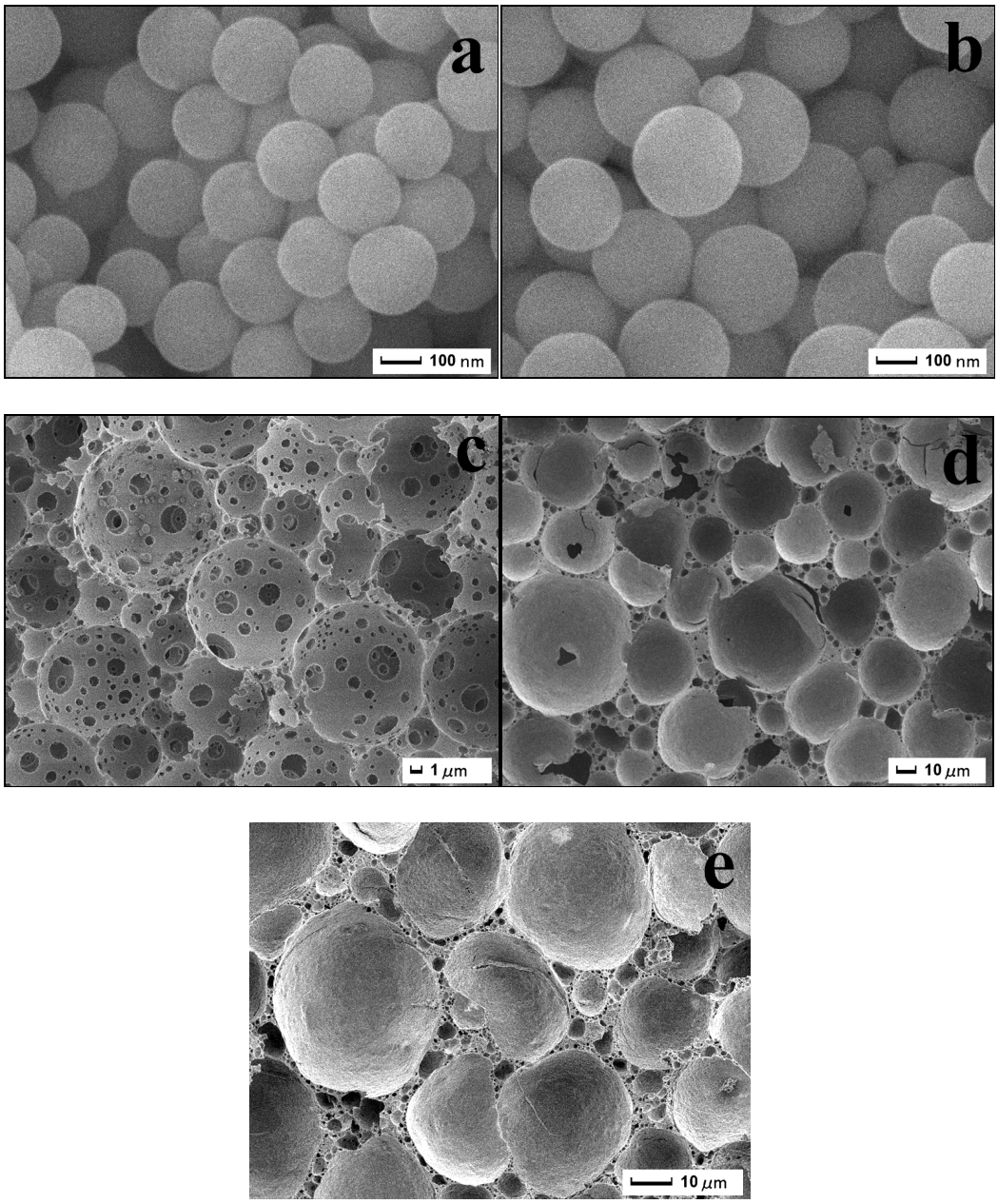

Fig. 2 SEM images of hydrophilic silica particles (a), hydrophobic silica particles (b), PDVB-SO_3H (c), PDVB-SS-SO_3H (d) and HC-PDVB-SS-SO_3H (e).

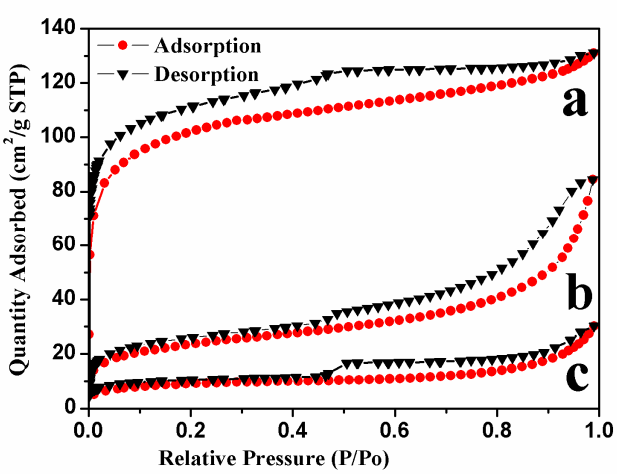

Fig. 3 Nitrogen adsorption-desorption isotherms of HC-PDVB-SS-SO_3H (a), PDVB-SS-SO_3H (b), and PDVB-SO_3H (c).

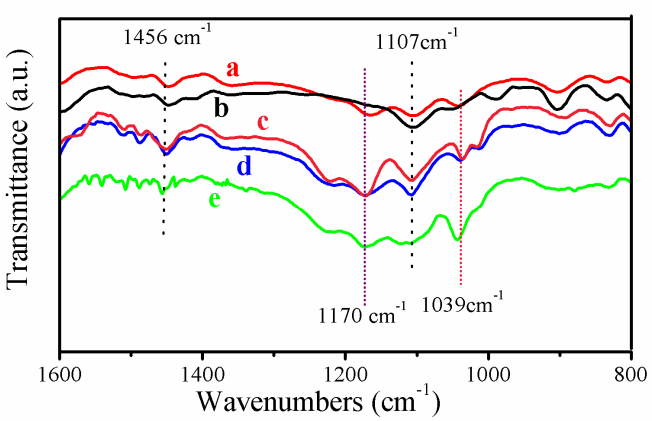

Fig. 4 FT-IR spectra of PDVB -SO_3H (a), PDVB (b), regenerated HC-PDVB-SS-SO_3H (c), HC-PDVB-SS-SO_3H (d) and PDVB-SS-SO_3H (e).

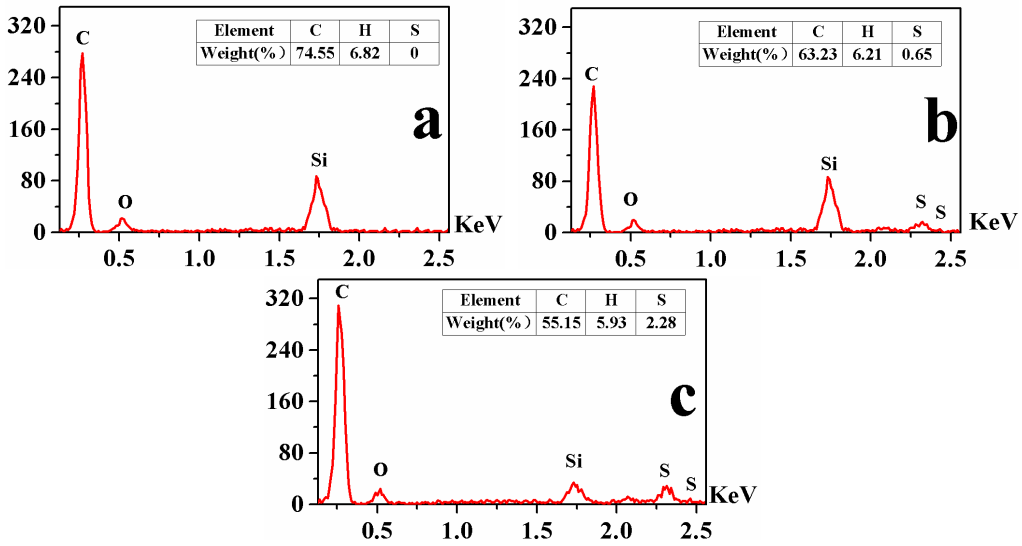

Fig. 5 Energy dispersive spectrometer (EDS) and element analysis of PDVB (a), PDVB-SO_3H (b) and PDVB-SS-SO_3H (c).

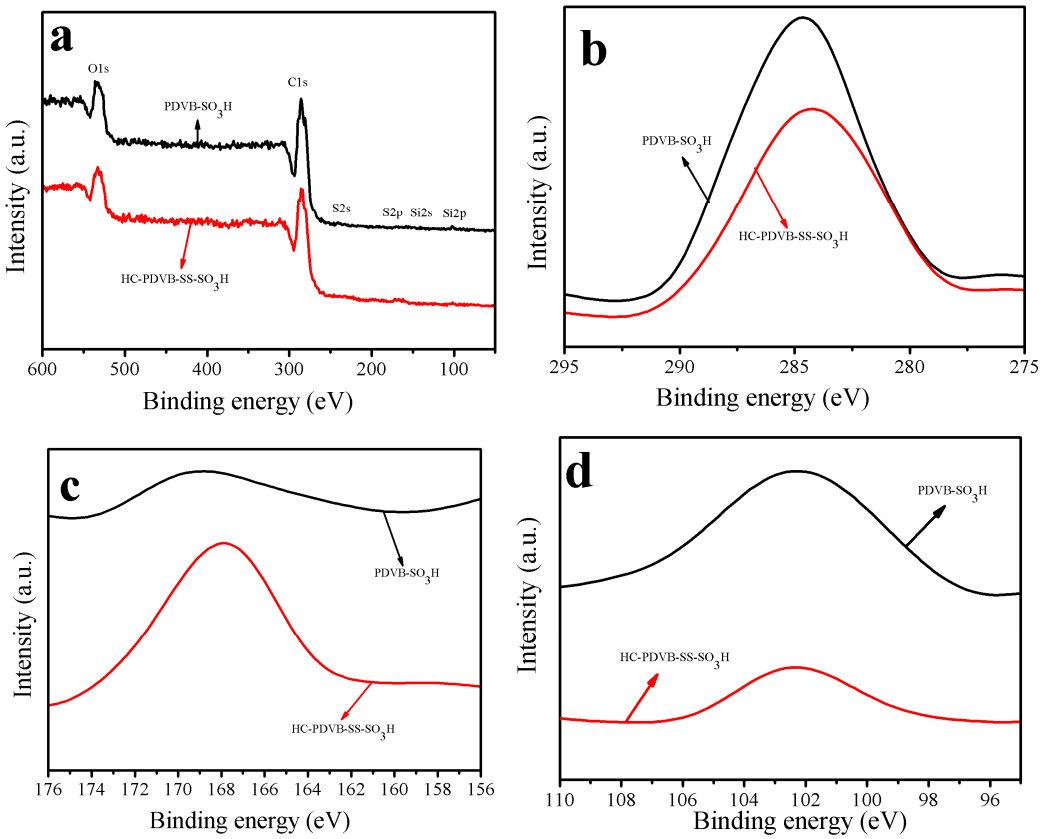

Fig. 6 X-ray photoelectron spectroscopy measurements of survey (a), C1s (b), S2p (c), Si2p (d) of PDVB-SO_3H and HC-PDVB-SS-SO_3H.

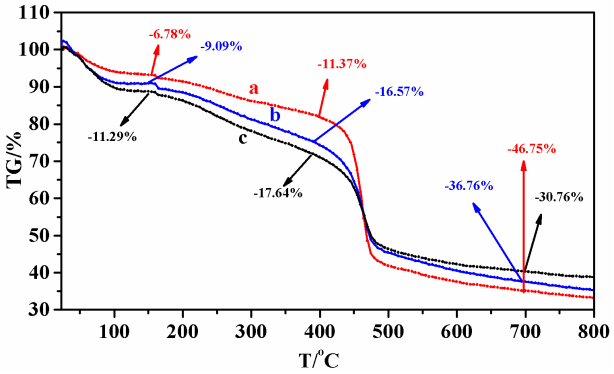

Fig. 7 TGA curves of PDVB-SO_3H (a), HC-PDVB-SS-SO_3H (b) and PDVB-SS-SO_3H (c).

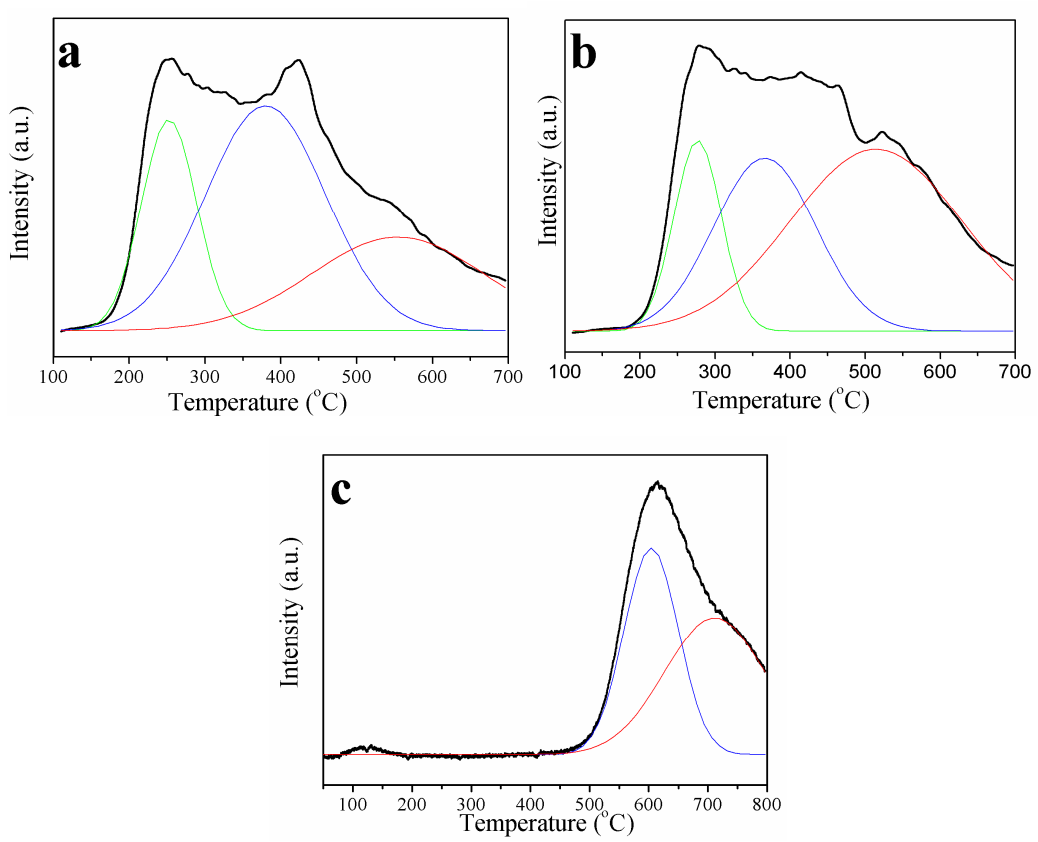

Fig. 8 NH_3-TPD curves of PDVB-SO_3H (a), PDVB-SS-SO_3H (b) and HC-PDVB-SS-SO_3H (c).

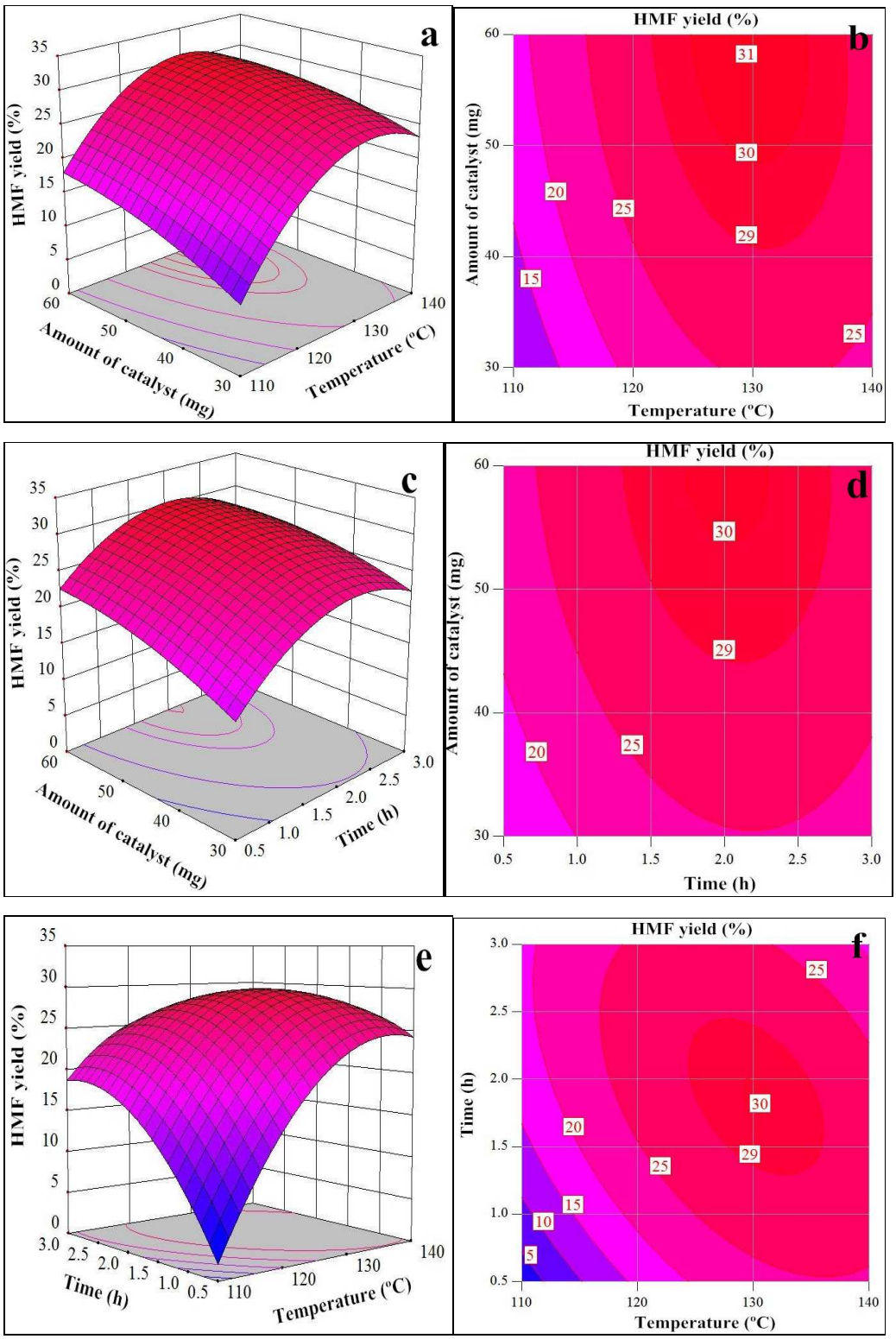

Fig. 9 Optimization of reaction conditions to cellulose to HMF using HC-PDVB-SS-SO_3H as the catalyst through response surface methodology. The effects of (a) and (b) amount of catalyst and temperature for 1.75 h; (c) and (d) reaction time and amount of catalyst at 125 ^oC; (e) and (f) reaction time and temperature with 45 mg of HC-PDVB-SS-SO_3H.

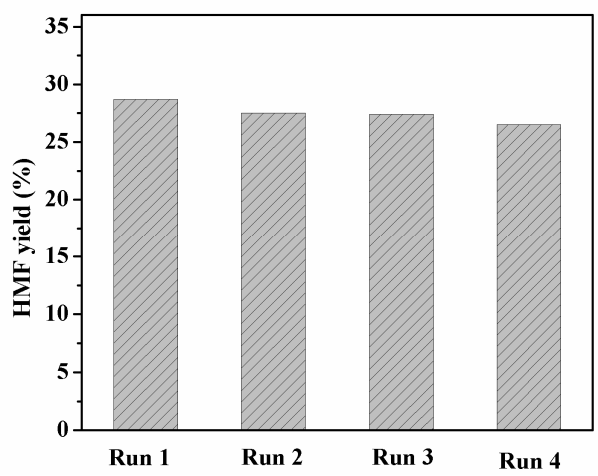

Fig. 10 Reusability of HC-PDVB-SS-SO_3H catalyst in the dehydration of cellulose into HMF in [EMIM]Cl under the optimized conditions: 125 °C, 45 mg of catalyst based on 0.10g of cellulose, 1.75 h, [EMIM]Cl 2.0 g.

Table 1 Recipes of W/O Pickering HIPEs.

Samples	External organic phase				Internal aqueous phase			
	DVB (mL)	AIBN (g)	Silica (g)	Span80 (mL)	Water (g)	K_2SO_4 (g)	KPS (g)	SS (g)
PDVB-SO_3H	3.0	0.04	0.3	0.4	16.8	0.08	0	0
PDVB-SS-SO_3H	3.0	0.04	0.3	0.4	16.8	0.08	0.04	0.2

Table 2 The porosity properties, acidic properties and catalytic efficiency of the catalysts.

Samples	V_t[a] ($cm^3\ g^{-1}$)	D_{BJH}[b] (nm)	S_{BET}[c] ($m^2\ g^{-1}$)	Acid strength (ºC)	Acid amounts (μmol g^{-1})	Total acidity (μmol g^{-1})	HMF (%)
PDVB-SO_3H	0.05	14.19	30.24	250 378 557	50 116 69	235	22.3[d]
PDVB-SS-SO_3H	0.13	10.67	80.06	285 369 518	49 95 169	313	25.2[d]
HC-PDVB-SS-SO_3H	0.20	5.94	323.95	604 706	104 133	237	28.9[e]

[a] V_t is the total pore volume determined at the relative pressure of 0.99.

[b] D_{BJH} is BJH pore diameter calculated by the desorption branches of the nitrogen sorption isotherms.

[c] S_{BET} is the BET specific surface area.

[d] The reaction condition are 2.0 h, 130 ^oC and 50 mg of catalyst.

[e] The reaction condition are 1.75 h, 125 ^oC and 45 mg of catalyst.

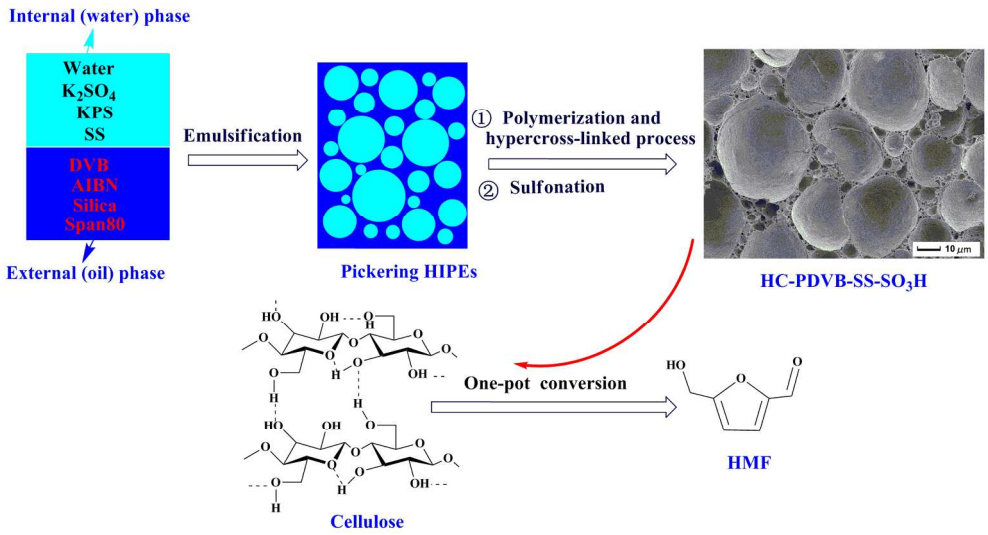

185x98mm (300 x 300 DPI)